Supporting Information

Red carbon dots directed biocrystalline alignment for piezoelectric energy harvesting

Wei Li [a, ⊥], Chuanfeng Wang [a, ⊥], Dingyun Shao [a, ⊥], Liang Lu [a], Jingjing Cao [a], Xuanlun Wang [b], Jun Lu [a, #, *], Weiqing Yang [a, *]

[a] Key Laboratory of Advanced Technologies of Materials, Ministry of Education, School of Materials Science and Engineering, Southwest Jiaotong University, Chengdu 610031, Sichuan, China

[b] College of Materials Science and Engineering, Chongqing University of Technology, Chongqing 400054, China

---

[⊥] These authors equally contributed to this work.
[#] Other used names Jun Lv and Jun Lyu.
[*] Corresponding authors. E-mail: junluprc@hotmail.com (J. Lu), wqyang@swjtu.edu.cn (W.Q. Yang).

Experimental Section

Characterization of Materials

Transmission electron microscopy (TEM) was conducted using a JEOL JEM-2100F instrument. Scanning electron microscope (SEM) images were acquired on a JSM-6330F apparatus. Laser scanning confocal microscopy (LSCM) was performed with a Nikon A1R+ microscope. X-ray diffraction (XRD) data were collected on a PANalytical X'pert PRO diffractometer. Attenuated total reflectance Fourier transform infrared (ATR-FTIR) spectra were recorded using a Nicolet iS20 spectrometer.

Photoluminescence (PL) spectra were recorded on a FLS980 spectrometer equipped with a 450 W xenon lamp. The 1931 CIE (International Commission on Illumination) system was used to calculate the chromaticity coordinates. The room-temperature absolute PL quantum yields (QYs) were measured using a calibrated integrating sphere attached to the Edinburgh FLS980 spectrometer (Figure S2, Supporting Information). To minimize the reabsorption effect, the sample solutions were diluted to an optical density of ca. 0.1 at the corresponding excitation wavelengths to obtain the accurate PL QY values [1]. The absolute PL QYs were calculated using the following formula [2, 3]:

$$PLQY = \frac{\int L_{emission}}{\int E_{solvent} - \int E_{sample}}$$

where $PLQY$ is the absolute quantum yield, $L_{emission}$ is the photon numbers of fluorescent emission of R-CQDs, and E_{sample} and $E_{solvent}$ are the photon numbers of excitation light for the excitation of R-CQDs and solvents (deionized water, aqueous acetic acid), respectively.

Pole figures were measured using a PANalytical Empyrean Series 2 X-ray diffraction system. The polar angle α ranged from 0^{o} to 60^{o}, and the azimuthal angle β from 0^{o} to 360^{o}, with a step of 5^{o} for both α and β. The measured incomplete pole figures were input into the Matlab toolbox MTEX, a free and open-source software for texture analysis and modeling, to calculate the complete pole figures based on orientation distribution function (ODF) [4, 5]. After that, the pole densities at specific locations were obtained from the complete pole figures. Detailed calculation methods of pole density can be found in references [4] and [5].

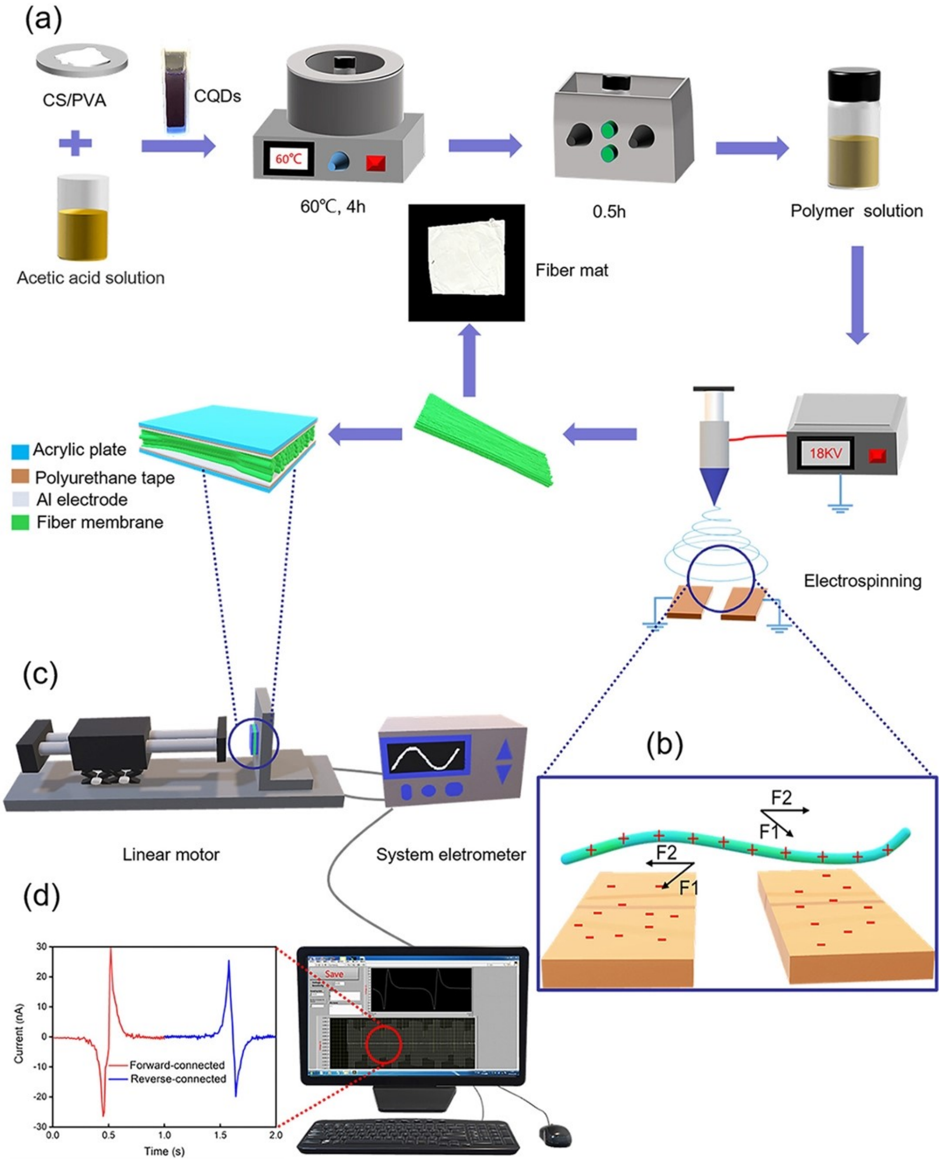

Figure S1. a) Schematic illustration of the fabrication process of uniaxially aligned CQDs/PVA/CS bionanofibers, and the composite structure of assembled bio-PNGs. The inset shows the digital image of a free-standing, and well-aligned electrospun nanofibrous film. b) Electrostatic force analysis of a charged hybrid bionanofiber during electrospinning. c) Schematic drawing of the impact measurement system for collecting electrical outputs generated by bio-PNGs. d) Output current signals of a CQDs/PVA/CS based bio-PNG when it is forward and reverse connected to the measurement system, respectively.

(a)

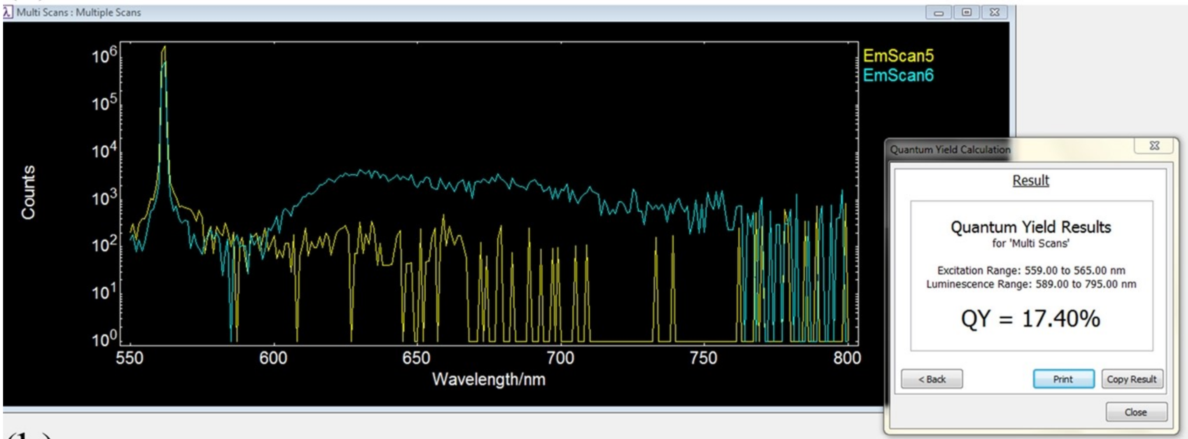

(b)

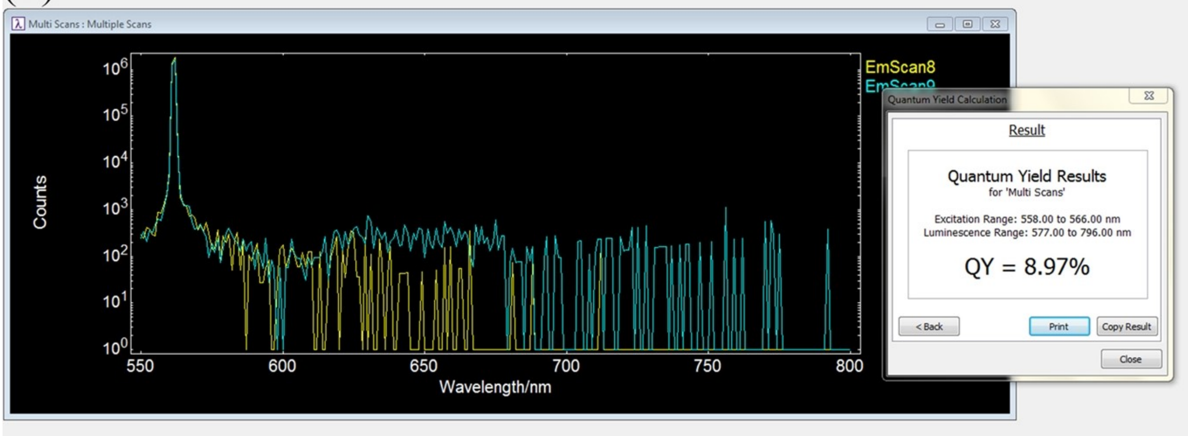

Figure S2. Room-temperature absolute PL QYs of a) R-CQDs and b) CQDs/PVA/CS, measured using a calibrated integrating sphere attached to an Edinburgh FLS980 spectrometer.

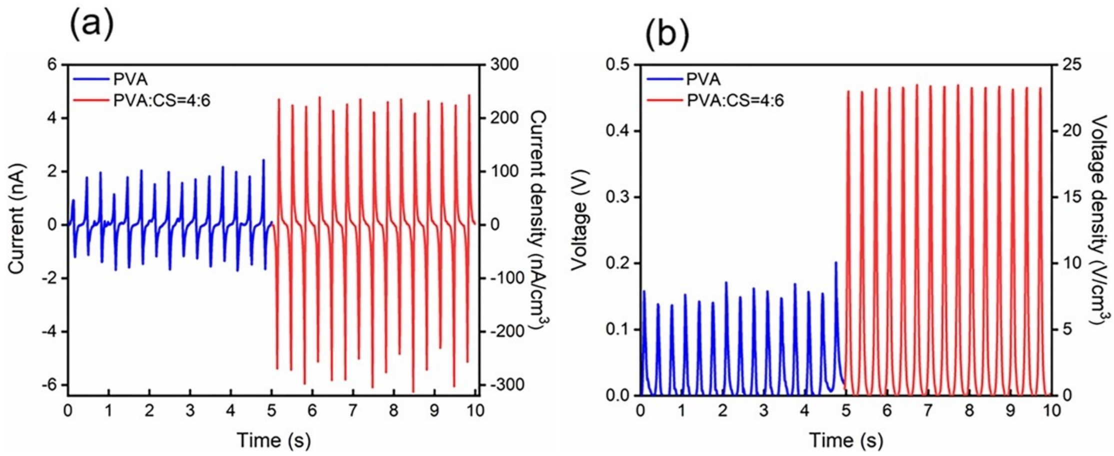

Figure S3. a) Short-circuit current and b) open-circuit voltage outputs of electrospun nanofibers of PVA and PVA/CS, respectively, generated at a stimulation frequency of 3.0 Hz and an applied force of 12 N. PNG size: 10 mm×10 mm×0.2 mm.

References

[1] C. Luo, C. Yan, W. Li, F. Chun, M. Xie, Z. Zhu, Y. Gao, B. Guo and W. Yang, Ultrafast thermodynamic control for stable and efficient mixed halide perovskite nanocrystals, *Adv. Funct. Mater.*, 2020, **30**, 2000026.

[2] J. Feng, Y. Ju, J. Liu, H. Zhang, X. Chen, Polyethyleneimine-templated copper nanoclusters via ascorbic acid reduction approach as ferric ion sensor, *Anal. Chim. Acta*, 2015, **854**, 153−160.

[3] Y. H. Liu, W. X. Duan, W. Song, J. J. Liu, C. L. Ren, J. Wu, D. Liu and H. L. Chen, Red emission B, N, S-co-doped carbon dots for colorimetric and fluorescent dual mode detection of Fe^{3+} ions in complex biological fluids and living cells, *ACS Appl. Mater. Interfaces*, 2017, **9**, 12663-12672.

[4] R. Hielscher and H. Schaeben, A novel pole figure inversion method: specification of the MTEX algorithm, *J. Appl. Crystallogr.*, 2008, **41**, 1024–1037.

[5] F. Bachmann, R. Hielscher and H. Schaeben, Texture analysis with MTEX – free and open source software toolbox, *Solid State Phenom.*, 2010, **160**, 63–68.